Journal Pre-proof

In differentiated HL-60 neutrophil-like cells, MRP1- (ABCC1-) mediated glutathione efflux stimulated by BzATP and P2X$_7$ receptor signalling regulates exosome release through nSMase activity

Erica Muriana Tintor, Anfal Sharif, Lúcia Moreno-Sánchez, Samuel Antwi-Baffour, Jameel M. Inal

Please cite this article as: E. Muriana Tintor, A. Sharif, L. Moreno-Sánchez, S. Antwi-Baffour, J.M. Inal, In differentiated HL-60 neutrophil-like cells, MRP1- (ABCC1-) mediated glutathione efflux stimulated by BzATP and P2X$_7$ receptor signalling regulates exosome release through nSMase activity, *Biochemical and Biophysical Research Communications*, https://doi.org/10.1016/j.bbrc.2026.153614.

This is a PDF of an article that has undergone enhancements after acceptance, such as the addition of a cover page and metadata, and formatting for readability. This version will undergo additional copyediting, typesetting and review before it is published in its final form. As such, this version is no longer the Accepted Manuscript, but it is not yet the definitive Version of Record; we are providing this early version to give early visibility of the article. Please note that Elsevier's sharing policy for the Published Journal Article applies to this version, see: https://www.elsevier.com/about/policies-and-standards/sharing#4-published-journal-article. Please also note that, during the production process, errors may be discovered which could affect the content, and all legal disclaimers that apply to the journal pertain.
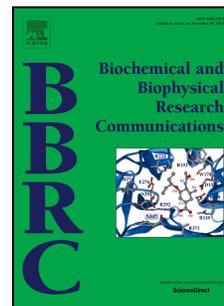
Title:

In differentiated HL-60 neutrophil-like cells, MRP1- (ABCC1-) mediated glutathione efflux stimulated by BzATP and P2X$_7$ receptor signalling regulates exosome release through nSMase activity

Short Running Title:

MRP1-mediated GSH efflux regulates P2X7-induced exosome release

Authors: Erica Muriana Tintor[1], Anfal Sharif[1], Lúcia Moreno-Sánchez[1], Samuel Antwi-Baffour[2,3] and Jameel M. Inal[1,2,4,*]

*Corresponding Author (Jameel M. Inal)

Affiliations:
[1]Cell Communication in Disease Pathology, London Metropolitan University, U.K.
[2]Cellular and Molecular Immunology Research Centre, London Metropolitan University, U.K.
[3]School of Biomedical and Allied Health Sciences, University of Ghana, Ghana
[4]School of Health, Medicine and Life Sciences, University of Hertfordshire, U.K.

ORCID Numbers:
Erica Muriana Tintor 0009-0009-8554-3429
Anfal Sharif 0009-0005-2921-2570
Lúcia Moreno-Sánchez 0009-0008-0513-4557
Samuel Antwi-Baffour 0000-0002-7653-1129
Jameel M. Inal 0000-0002-7200-0363

Keywords:

Extracellular Vesicles: Exosome biogenesis; Neutrophils; redox regulation; purinergic signalling

In differentiated HL-60 neutrophil-like cells, MRP1- (ABCC1-) mediated glutathione efflux stimulated by BzATP and P2X$_7$ receptor signalling regulates exosome release through nSMase activity

Abstract

Exosomes are endosome-derived extracellular vesicles (EVs) playing key roles in immune regulation and inflammatory signalling, yet with poorly defined mechanisms of biogenesis. We investigated how purinergic signalling and redox regulation intersect, controlling exosome formation in neutrophil-like cells (NLCs) differentiated from the HL-60 cell line. Differentiated NLCs displayed hallmark neutrophil features, including increased CD11b expression, reduced CD71, enhanced phagocytosis, robust reactive oxygen species generation, and cell-cycle arrest. CD63-positive exosomes released from NLCs fulfilled MISEV 2023 criteria, exhibiting typical morphology, density, and size distribution.

Stimulation with the P2X$_7$R agonist BzATP induced a rapid, dose-dependent increase in exosome release correlating strongly with depletion of intracellular glutathione (iGSH) and activation of neutral sphingomyelinase (nSMase). Pharmacological inhibition of nSMase abrogated BzATP-induced exosome release, implicating ceramide-dependent intraluminal vesicle formation. Mechanistically, BzATP activated PI3K/AKT signalling, leading to stimulation of the ABC transporter MRP1/ABCC1, enhanced efflux of GSH, and a concomitant rise in extracellular GSH. Inhibition of PI3K/AKT or MRP1 prevented iGSH efflux, reduced nSMase activity, and significantly attenuated exosome secretion.

These findings define a previously uncharacterized pathway in NLCs whereby extracellular ATP acts as a danger signal triggering PI3K/AKT–MRP1–dependent redox gating of nSMase activity, thereby driving rapid exosome biogenesis. This mechanism provides insight into how neutrophils translate inflammatory cues into vesicle-mediated communication and highlights potential therapeutic targets to modulate pathological neutrophil-driven inflammation.

1. Introduction

Extracellular vesicles (EVs) are membrane-bound nanostructures mediating intercellular communication by transferring bioactive molecules such as proteins, lipids, and nucleic acids between cells [1]. Among EV subtypes, exosomes originate from the endosomal system being formed through inward budding of endosomal membranes, generating intraluminal vesicles (ILVs) within multivesicular bodies (MVBs). Upon fusion of MVBs with the plasma membrane (PM), these ILVs are released as exosomes, in contrast with microvesicles (MVs), which bud directly from the PM [2].

Exosomes maintain cellular homeostasis and orchestrate physiological processes, while also contributing to pathological states such as infection, cancer, and autoimmune disorders [3]. Their ability to deliver diverse cargo—including lipids, proteins, and microRNAs—to recipient cells via receptor-mediated interactions or membrane fusion underscores their importance in immune regulation and disease progression. Beyond natural functions, exosomes have attracted interest as therapeutic vehicles for targeted delivery of drugs or genetic material [3]. To harness this potential, understanding molecular mechanisms governing exosome biogenesis, especially in neutrophils where this remains unclear, is essential for incorporating therapeutic payloads and modulating vesicle release.

Despite advances in EV biology and understanding of exosome biogenesis in macrophages [2], signalling pathways regulating ESCRT-independent exosome secretion in neutrophils remain incompletely defined [4]. Neutrophils, key effectors of innate immunity, express functional $P2X_7$ receptors ($P2X_7R$) on their PM which, upon activation by the agonist BzATP, induce calcium influx, potassium efflux, respiratory burst, and membrane pore formation [5]. Neutrophil-like cells differentiated from the HL-60 promyelocytic leukaemia line provide a robust experimental model to study these processes, closely mimicking primary neutrophil behaviour [6].

Previous studies in macrophages have implicated extracellular ATP (eATP) and $P2X_7R$ signalling in exosome biogenesis through activation of neutral sphingomyelinase (nSMase), an enzyme negatively regulated by intracellular glutathione (iGSH) [7,2]. Depletion of iGSH increases Reactive Oxygen Species (ROS). By causing lysosomal dysfunction that would otherwise limit MVB accumulation, MVB numbers and exosome secretion increase [8]. Increased extracellular GSH (eGSH) suggests active transport by ATP-binding cassette transporters, including MRP1/ABCC1. MRP1 likely contributes to this pathway, as its inhibition reduces both GSH efflux and exosome release.

Extracellular ATP is a danger signal for neutrophils, activating their P2 receptors, that bind ATP, ADP, and UTP [5]. The 1-3 mM concentrations of eATP found locally, released from damaged cells, are sufficient to activate $P2X_7Rs$ triggering cell death pathways, inflammation (IL-1β release) and ROS production in neutrophils In this study we used BzATP which has a higher affinity than ATP for $P2X_7Rs$, at concentrations up to 300 µM, to ensure maximal $P2X_7R$ activation and downstream proinflammatory responses. This concentration also overwhelms the anti-inflammatory signalling triggered by $P2Y_{11}$ receptors (which can be triggered by low µM concentrations of eATP). Neutrophil-like cells differentiated from the promyelocytic leukaemia cell line, HL-60, were used as they represent an excellent model, mimicking primary neutrophils.

Building on these insights, the current study aimed to elucidate how purinergic signalling and redox regulation intersect to control exosome biogenesis in NLCs. Specifically, the $P2X_7R$-mediated activation of PI3K/Akt signalling was investigated, its influence on ABC transporter activation, and the downstream effects on nSMase activity and exosome formation. By advancing our understanding of neutrophil vesiculation, novel targets for therapeutic modulation of inflammatory responses can be identified.

2

2.   Materials and Methods

2.1 Differentiation of HL-60 cells to Neutrophil-like cells (NLCs)

The human myeloid HL-60 cells were obtained from HPA and maintained in RPMI 1640 medium with 5% EV-depleted FBS (120,000 ×g/18h, then ultrafiltration (amicon, 100 kDa MWCO, 3,500 ×g/60 min) and 100 U/ml penicillin, 100 µg/ml streptomycin at 37 °C in a humidified atmosphere (5% CO_2). The cells were split every 2-3 days. After maintaining the cells for 3 weeks, differentiation to NLCs was induced. HL-60, (10^5 cells/ml) were treated with 1 µM all-trans retinoic acid (ATRA) and 1% dimethyl sulfoxide (DMSO) for 5 days. Once differentiated, cells no longer needed splitting and were used within a further 5 days.

2.2 Phagocytosis assay and cell cycle analysis

These are described in details in Supplementary Information. Essentially, phagocytosis by NLCs was quantified by flow cytometry using pHrodo Green E. coli BioParticles, with uptake indicated by increased fluorescence and reported as the percentage of pHrodo-positive cells relative to controls.

Cell cycle distribution of HL-60 cells was determined by propidium iodide staining of DNA followed by flow cytometric analysis to classify cells into G0/G1, S, and G2/M phases based on DNA content [12].

2.3 Isolation of exosomes

Firstly small EVs were isolated by differential centrifugation. The NLC cell culture supernatant of BzATP-treated cells (for 2h) was centrifuged (160 ×g/10 min/4 °C). The supernatant was centrifuged (3,000 ×g /30 min/4 °C) and new supernatant filtered through a 0.22 µm pore size filter before centrifugation (25,000 ×g /30 min/4 °C) and final centrifugation (100,000 ×g /60 min/4 °C) with a final wash in 0.22 µm pore-filtered PBS, re-centrifugation and resuspension in a minimal volume. Exosomes were specifically isolated by immunoaffinity (IA) using the Tetraspanin Exo-Flow Capture kit (System Biosciences). This was carried out according to the manufacturer's protocol. Essentially, the CD63-biotin antibody was coupled to the magnetic streptavidin beads (CD63-MBs). These CD63-MBs were then used to collect exosomes (or CD63-positive EVs) from the small EVs (150 µg) isolated by differential ultracentrifugation/ultrafiltration. After washing off unbound material, exosomes were eluted with exosome elution buffer. Exosomal buoyant density was determined by OptiPrep density gradient centrifugation. By combining IA with nanosight tracking analysis (NTA) we were able to monitor exosome biogenesis in real-time, obviating the need for a reporter system.

2.4 Nanosight Tracking Analysis (NTA)

To measure EV sample concentration and distribution profiles of EV diameter, the NanoSight NS300system (Malvern Instruments Ltd, UK) was used as described previously [9]. CD63-enriched exosomes were collected from 3 different samples of NLCs, diluted 500-fold in 1 ml of DPBS and injected into the instrument. Videos (5 × 1 min) were recorded as per the manufacturer's instructions (between 17.5 and 19.5 °C). The EV concentration and size profile was derived using the NanoSight Software NTA 3.2 (Malvern).

2.5 SDS-Polyacrylamide Gel Electrophoresis and western Blotting

Protein extraction and protein assays were carried out as described previously [10]. Essentially, NLC exosomal proteins were obtained by lysing exosomes in cold RIPA buffer (Sigma) containing protein inhibitors (Sigma) for 60 min on ice followed by centrifugation (16,250 ×g /20 min/4 °C). Protein concentrations were measured by BCA protein Assay or by NanoOrange (both Thermo Scientific) as

3

described previously [11].   For SDS-PAGE, samples were denatured in β-mercaptoethanol (95 °C/10 min); for deglycosylation, SDS was neutralised with NP-40 and 10 μg protein typically deglycosylated with 500 units of PNGaseF (37 °C/16 h). Western blotting was carried out using the Mini-PROTEAN tetra system on 4-20% TGX gels (Bio-Rad) as outlined previously [9] and transferred to nitrocellulose by semi-dry electrotransfer. The mouse antibodies used to probe the membrane were: anti-CD63 (1/1,000; Abcam, ab271286), anti-LAMP-2 (1/500; Abcam; ab25631), anti-Alix (1/1,000; Abcam; ab117600); anti-GM130 (1/500; Sigma-Aldrich, MABT1363). A rabbit polyclonal anti-P2X$_7$R recognising an extracellular domain was from Alomone labs (1/500; APR-008) and anti-β-actin (1/1,000; Abcam, ab8226). The secondary antibodies used were anti-mouse and anti-rabbit HRP-conjugated antibodies (Bio-Rad) used at a 1/3,000 dilution, the blot then being visualised using chemiluminescence (ECL) and the UVP digital imaging system.

2.6 Immuno-Transmission Electron Microscopy

Paraformaldehyde-fixed exosomes were labelled with immunogold by first placing on a formvar carbon-coated nickel grid. They were blocked in 5% BSA/PBST and then incubated for 1h in with mouse monoclonal against human CD9 used at a 1/100 dilution (BD Pharmingen, Clone M-L13). Six 10 minute washes was followed by incubation in the secondary antibody (5 nm gold particle anti-mouse antibody (1/50 dilution). The grid was washed in PBS, distilled water and negative staining carried out with 2% uranyl acetate (Agar Scientific, UK). The grids were visualised using a JEM-1200 EX II electron microscope (JEOL, Peabody, MA), digital images, up to 40,000 magnification being obtained on an AMT digital camera.

2.7 Assay for intracellular calcium

This was carried out as described previously [11]. In brief, NLCs (5 × 10^4 cells/well) were seeded into black-walled 96-well plates. After exposure to LPS (300 ng/ml for 3h) cells were washed and resuspended in phosphate buffered saline (PBS) loaded with 2 μM Fura 2-AM and 2 mM probenecid (30 min/ 37 °C. After washing off the loading solution and resuspending in PBS, steady state readings were taken on a fluorescent plate reader (λ_{ex}340/380 nm, λ_{em}540 nm) for 10 min. Upon addition of BzATP (300 μM) readings were measured for 50 min. Maximum fluorescence readings were obtained by lysing cells in 1% Triton X-100.

2.8 Intracellular and Extracellular GSH assays

The details of these methods are in the Supplementary Information. Essentially, intracellular reduced glutathione (iGSH) was quantified using a competitive ELISA on 5-Sulfosalicylic Acid- (SSA-) extracted cell lysates from ~1×10^6 cells, with concentrations derived from a standard curve and normalised to protein content.

Extracellular GSH in clarified culture medium was measured by a luminescence-based assay after reaction with GSH-Glo reagents, with background subtraction and standard-curve conversion to determine eGSH levels.

2.9 nSMase Enzyme Activity Assay and Measurement of Intracellular ROS

These assays are detailed in Supplementary Information. Essentially, nSMase activity was quantified using a coupled enzymatic colorimetric assay in which sphingomyelin hydrolysis generated a blue product measured at 595 nm; activity was calculated from a standard curve, normalised to protein content, and expressed relative to untreated controls.

Intracellular ROS in PMA-treated HL-60 cells was measured by H_2DCFDA staining followed by flow cytometry, where oxidation to fluorescent DCF (λmax 530 nm) was quantified as median fluorescence intensity and compared between groups.

2.10 Flow cytometric analysis of HL-60 cells and human peripheral neutrophils

Flow cytometry was carried out as described previously [11]. Briefly, HL-60 cells, differentiated or not, were incubated in Fc receptor blocking solution for 20 min at room temperature before staining with anti-CD71 and anti-CD11b. Cells ($5x10^5 - 10^6$ cells/mL) washed twice in PBS, were incubated for 1h, in the dark, with FITC-labelled anti-CD71 (MEM-75, Thermo Fisher) and FITC-labelled mouse anti-human CD11b antibody (clone ICRF44; Bio-Rad). After washing analysis was with the Guava EasyCyte 8HT flow cytometer.

2.11 Statistical analyses

Data are presented as mean ± SEM, $p<0.05$ considered statistically significant. Statistical analyses used GraphPad Prism (version 10.6.1 for Windows). To evaluate the effects of BzATP on iGSH and EVs, a two-way analysis of variance (ANOVA) was conducted with Tukey's post-hoc test. The relationship between BzATP and nSMAse activity was assessed using simple linear regression. For BzATP and nSMAse activity, dose-response data were fitted to a four-parameter logistic (4PL) curve using nonlinear regression with the least-squares method to determine IC50 values.

3. Results

3.1 Characterisation of neutrophil-like cells (NLCs) differentiated from promyelocytic HL-60 cells

To study exosome biogenesis in neutrophils, and to overcome problems with donor variability and short lifespan, rather than primary neutrophils, NLCs were chosen to ensure stable populations. To differentiate into NLCs, HL-60 cells were treated with ATRA plus DMSO for 3 and 5 days and showed increased expression of CD11b and decreasing expression of CD71 (Fig. 1A). The NLCs had increased capacity to phagocytose pHrodo Green E. coli particles (Fig. 1B and representative histograms in Fig. 1C). Upon PMA treatment, there was greatly increased ROS in NLCs compared to undifferentiated HL-60 (Fig. 1D and E) and decrease in S-phase (Fig. 1F). The NLCs were also confirmed to express $P2X_7R$ at increased levels compared to the undifferentiated HL-60 (Fig. 1G) and also increased expression when LPS-stimulated (Fig. 1H). To demonstrate their functionality, LPS-primed NLCs treated with BzATP resulted in an increase in Ca^{2+} influx, which could be inhibited with the $P2X_7R$ antagonist, A740003 (Fig. 1I).

3.2 BzATP stimulation of NLCs and associated reduction of iGSH coupled with increased nSMAse activity and exosomal release

The CD63-enriched EVs (henceforth called exosomes) were isolated from NLCs by differential centrifugation and immunocapture using biotinylated anti-CD63 capture antibodies conjugated to streptavidin-conjugated magnetic beads. They were visualised by immuno-gold transmission electron microscopy using anti-CD9 (Fig. 2A). This revealed CD63-expressing "cup-shaped" EVs (a typical, though artefactual morphology of exosomes seen in TEM). NTA gave a peak modal size of 112 nm and range of 30-168 nm (Fig. 2B). Their buoyant density was 1.10-1.12 g/ml (Fig. 2C). For CD63, the NLCs (differentiated HL-60) showed hyperglycosylation (and increased expression of deglycosylated CD63) compared to undifferentiated HL-60 cells (Fig. 2D). The exosomes released from these cells were confirmed positive for EV markers (CD63 and Alix) but not the negative control Golgi apparatus marker, GM130 (Fig. 2E). Purity was confirmed with a total protein: particle number ratio <10^{10} particles/µg protein.

Upon treatment of NLCs for 30 min with increasing concentrations of BzATP (eATP being a damage-associated molecular pattern (DAMP)), a strong positive correlation was found with exosome release (r=0.948, p=0.02) which was concomitant with a strong negative correlation (r=-0.984, p=0.01) with iGSH (Fig. 2F). Since iGSH is known to inhibit nSMAse [13] which is implicated in ILV formation in MVBs [14], we surmised that increasing BzATP (and therefore limiting iGSH) would lift inhibition of nSMAse, thus increasing its activity as demonstrated in Fig. 2G. To confirm nSMase-specific activity, we incorporated a specific nSMase inhibitor, GW4869, in NLCs similarly stimulated with BzATP (Fig. 2G (inset)).

3.3 iGSH is exported in a MK-571-inhibitable manner in response to BzATP resulting in a drop of iGSH and concomitant increase in exosomal release

BzATP-mediated $P2X_7R$ and $P2Y_{11}R$ signalling activates MRP1 through PI3K/AKT stimulation of aerobic glycolysis and production of ATP within minutes, which MRP1 needs, to actively pump substrates out of the cell [14]. We were able to demonstrate this in NLCs by the efflux of calcein-AM with increasing BzATP (Fig. 3A) and that this could be inhibited by MK-571 (Fig. 3A). The BzATP/PI3K/AKT-activated MRP1-mediated removal of iGSH from the cell should therefore result in increased eGSH. This was confirmed by demonstrating 150 µM BzATP significantly increasing eGSH, in a MK-571-inhibitable manner (Fig. 3C). We also found that two drugs affecting MRP1, MK-2206 which inhibits PI3K/AKT and therefore activation of MRP1 and MK-571 which blocks active MRP1, both inhibited EV release from BzATP-stimulated NLCs (Fig. 3C and E). To once more show decreasing iGSH with increasing concentrations of applied extracellular BzATP, it was then further showed that MK-571 could lessen this reduction in iGSH (Fig. 3D) and reduce the increase of exosome release (Fig. 3E).

4. Discussion

Differentiation of HL-60 cells with ATRA+DMSO yielded NLCs exhibiting hallmark features of mature neutrophils including increased (CD11b) and decreased (CD71) abundance, enhanced phagocytic capacity, heightened PMA-induced ROS generation, and cell-cycle arrest. NLCs provide a robust surrogate for primary neutrophils in vesicle biogenesis studies. Exosomes purified from NLCs fulfilled ISEV-accepted criteria (MISEV 2023) [15] including CD63/Alix positivity with GM130 exclusion, "cup-shaped" morphology by immuno-TEM of CD63-positive exosomes, and a peak modal diameter near 112 nm by NTA.

4.1 Purinergic, redox, and sphingolipid coupling in exosome biogenesis

A key observation was the rapid, dose-dependent increase in exosome release after 30 min of BzATP treatment, tightly inversely correlated with iGSH levels. As reduced iGSH is a known endogenous inhibitor of nSMase, its depletion would be expected to disinhibit nSMase, increase ceramide production, and promote intraluminal vesicle (ILV) formation within MVBs, thereby driving exosome secretion [16,17,18,19]. Consistent with this model, pharmacological nSMase blockade with GW4869 curtailed BzATP-evoked vesicle release, implicating nSMase activity as a necessary step in the pathway [16].

Mechanistically, eATP (a prototypic DAMP) engages purinergic receptors, notably $P2X_7R$ (but also $P2Y_{11}$ in neutrophils), to initiate signalling programs intersecting with lipid metabolic enzymes needed for vesicle biogenesis [20]. Our data place redox regulation at the centre of this cascade: BzATP stimulation lowers cytosolic iGSH while increasing eGSH, and the magnitude of exosome release positively tracks this GSH efflux. Because ceramide-dependent ILV formation is sensitive to the iGSH/nSMase axis, the ATP-driven exporter-mediated loss of iGSH functions as a rapid molecular switch to gate nSMase activity and exosome output.

4.2 Evidence for a PI3K/AKT–MRP1 (ABCC1) arm upstream of iGSH efflux

Upstream of nSMase, the transporter and signalling data converge on a PI3K/AKT–MRP1 (ABCC1) efflux mechanism. First, BzATP increased calcein-AM efflux, an observation consistent with MRP1 activity, and MK-571 (an MRP1 inhibitor) blocked this effect supporting the role of MRP1 in ATP-dependent efflux processes [21]. Second, MK-571 attenuated the BzATP-induced depletion of iGSH and the rise in eGSH [21]. Third, pharmacologic inhibition of AKT (MK-2206) or direct MRP1 blockade (MK-571) reduced exosome release. Our results showed in neutrophils, that BzATP activates $P2X_7R$ and PI3K/AKT signalling, in turn stimulating MRP1-mediated iGSH efflux and providing relief of nSMase inhibition. The subsequent accumulation of ceramide resulted in exosome biogenesis. While PI3K/AKT modulation of ABC transporters is well documented (particularly for ABCG2 localization and activity) and MRP1 is recognized for transporting iGSH and iGSH-conjugates, further genetic validation would strengthen the specific link to neutrophil-lineage cells.

4.3 Biological significance and potential translation

The delineated pathway underscores how NLCs can transduce an ATP danger signal into fast, post-translational control of vesicle biogenesis via redox gating. By exporting iGSH through MRP1, cells swiftly lift nSMase inhibition and trigger ceramide-dependent ILV budding, enabling rapid exosome release without requiring de novo gene expression. In inflammatory microenvironments enriched in eATP, such a mechanism could amplify intercellular communication through exosomal cargoes (proteins, lipids, miRNAs) and potentially modulate innate responses and tissue outcomes [22].

Neutrophil exosomes are a key element in hyperinflammatory disease. They transport inflammatory cargo (miR155, leukotriene B4) which further activates neutrophils and other immune cells and damaging enzymes (cathepsin G, MMP-9, proteinase 3 and neutrophil elastase) leading to organ dysfunction. This perpetuates chronic inflammation preventing tissue repair. Dangerous hyperinflammation with excessive neutrophil activity and NETosis (release of Neutrophil Extracellular Traps), is part of the pathology of various diseases including sepsis (severe infection), autoimmune diseases, chronic lung diseases (COPD) and certain cancers. From a translational perspective, pharmacological targeting of PI3K/AKT, MRP1, or nSMase offers testable strategies to dampen excessive neutrophil vesiculation in hyperinflammatory states, while redox-modulating agents (e.g., GSH donors) might suppress ATP-evoked exosome release [23].

4.4 Conclusion

Our findings summarised in Figure 4, support a framework in which BzATP-triggered purinergic signalling activates a PI3K/AKT–MRP1 axis to export iGSH, relieving nSMase inhibition and promoting ceramide-driven ILV formation and exosome release from NLCs. Going forward, the pathway's pharmacological inhibition, and integration of damage-associated ATP with redox-sensitive lipid biogenesis highlight points for modulating neutrophil vesiculation in inflammation.

Acknowledgements

Figure Legends

Fig. 1. (A) Flow cytometry for expression of CD71 and CD11b was carried out after 0, 3 and 5 days of treatment of HL-60 cells with ATRA + DMSO using a Guava EasyCyte 8HT flow cytometer. (B), Percentage phagocytosis of pHrodo Green E. coli particles by NLCs (HL-60 cells differentiated for 5 days with ATRA + DMSO) compared to undifferentiated HL-60 cells, was measured using the FACSCanto II flow cytometer, representative histograms of engulfed particles measured as pHrodo green fluorescence intensity shown in (C). ROS production was measured as H2DCFDA fluorescence (MFI) on HL-60 and NLCs upon PMA stimulation (D) with representative histograms in (E). Cell cycle analysis (% S phase) for differentiated HL-60 after 3 and 5 days (F) and expression of $P2X_7R$ in HL-60 and NLCs by western blotting (G) showing band intensities normalised to β-actin, made relative to undifferentiated control, and by flow cytometry (H) and immunofluorescence microscopy (inset, H). Ca^{2+} uptake was monitored using Fura 2-AM upon adding BzATP to LPs-stimulated NLCs (I). Data are presented as mean ± SEM. Statistical significance was determined using an unpaired, two-tailed Student's t-test (n=5 per group).

Fig. 2. Immuno-transmission electron microscopy was used to reveal isolated CD63-positive exosomes, using anti-CD9 and 5 nm immunogold-conjugated secondary antibody (A) and their size range and peak modal size measured by NTA (B). Optiprep density gradient centrifugation showed the exosomes to have a density of 1.10-1.12 g/ml (C). Western analysis showed 5-day differentiated HL-60 cells (NLCs) to have increased expression of CD63 (D); image J 1.52p was used to calculate fold-changes of deglycosylated CD63 expression, band intensities normalised to β-actin and compared relative to control. The exosomal expression of EV markers was also compared with their parental cells (E). NLCs exposed to increasing BzATP concentrations up to 300 μM, were assayed for iGSH and concentration of released exosomes (F) and nSMAse activity (G) and in the presence of nSMAse inhibitor, GW4869 (F, inset). For (D) and (E) bars represent the mean ± SEM of n=3 independent biological replicates. Relationship between BzATP and iGSH, exosomes and nSMAse activity shown by linear regression fit, statistical significance of correlation indicated by R^2 or r value and associated p-value.

Fig. 3. In (A), calcein-AM was measured in NLCs exposed to BzATP up to 150 μM, the filled red circle indicating the inhibitory effect of MK-571 on calcein-AM export. Increased eGSH (B) and exosome release (C) was measured upon BzATP stimulation of NLCs (also in the presence of inhibitors MK-571 and MK-2206). With increased expression of BzATP, iGSH (D) and exosome release (E) was assayed (also in the presence of MRP1-blocking MK-571) with increasing BzATP. Data are presented as mean ± SEM of n=3 independent biological replicates. Statistical significance was determined by 2-way ANOVA followed by Tukey's post-hoc for pairwise comparisons between BzATP treated in the absence or presence of MK-571 and comparisons against the untreated control. Significance is indicated as *p < 0.05, **p < 0.01, and ***p < 0.001.

Fig. 4. Model for MRP1- (ABCC1-) mediated glutathione efflux in neutrophil-like cells in which $P2X_7Rs$ stimulated by BzATP regulates nSMAse activity and exosome release.

References

[1] De Sousa KP, Rossi I, Abdullahi M, Ramirez MI, Stratton D, Inal JM. Isolation and characterization of extracellular vesicles and future directions in diagnosis and therapy. Wiley Interdiscip Rev Nanomed Nanobiotechnol. 2023 Jan;15(1):e1835. doi: 10.1002/wnan.1835.

[2] Wang W, Qiao S, Kong X, Zhang G, Cai Z. The role of exosomes in immunopathology and potential therapeutic implications. Cell Mol Immunol. 2025 Sep;22(9):975-995. doi: 10.1038/s41423-025-01323-5.

[3] Wang Y, Xiao T, Zhao C, Li G. The Regulation of Exosome Generation and Function in Physiological and Pathological Processes. Int J Mol Sci. 2023 Dec 23;25(1):255. doi: 10.3390/ijms25010255.

[4] Aheget H, Tristán-Manzano M, Mazini L, Cortijo-Gutierrez M, Galindo-Moreno P, Herrera C, Martin F, Marchal JA, Benabdellah K. Exosome: A New Player in Translational Nanomedicine. J Clin Med. 2020 Jul 26;9(8):2380. doi: 10.3390/jcm9082380.

[5] Karmakar M, Katsnelson MA, Dubyak GR, Pearlman E. Neutrophil P2X7 receptors mediate NLRP3 inflammasome-dependent IL-1β secretion in response to ATP. Nat Commun. 2016 Feb 15;7:10555. doi: 10.1038/ncomms10555.

[6] Bhakta SB, Lundgren SM, Sesti BN, Flores BA, Akdogan E, Collins SR, Mercer F. Neutrophil-like cells derived from the HL-60 cell-line as a genetically-tractable model for neutrophil degranulation. PLoS One. 2024 Feb 7;19(2):e0297758. doi: 10.1371/journal.pone.0297758.

[7] Raffaele S, Lombardi M, Verderio C, Fumagalli M. TNF Production and Release from Microglia via Extracellular Vesicles: Impact on Brain Functions. Cells. 2020 Sep 23;9(10):2145. doi: 10.3390/cells9102145.

[8] Zhang W, Liu R, Chen Y, Wang M, Du J. Crosstalk between Oxidative Stress and Exosomes. Oxid Med Cell Longev. 2022 Aug 30;2022:3553617. doi: 10.1155/2022/3553617.

[9] Antwi-Baffour S, Malibha-Pinchbeck M, Stratton D, Jorfi S, Lange S, Inal J. Plasma mEV levels in Ghanain malaria patients with low parasitaemia are higher than those of healthy controls, raising the potential for parasite markers in mEVs as diagnostic targets. J Extracell Vesicles. 2019 Dec 18;9(1):1697124. doi: 10.1080/20013078.2019.1697124.

[10] Jorfi S, Ansa-Addo EA, Mariniello K, Warde P, Bin Senian AA, Stratton D, Bax BE, Levene M, Lange S, Inal JM. A Coxsackievirus B1-mediated nonlytic Extracellular Vesicle-to-cell mechanism of virus transmission and its possible control through modulation of EV release. J Gen Virol. 2023 Sep;104(9). doi: 10.1099/jgv.0.001884.

[11] Ansa-Addo EA, Pathak P, McCrossan MV, Volpato Rossi I, Abdullahi M, Stratton D, Lange S, Ramirez MI, Inal JM. Monocyte-derived extracellular vesicles, stimulated by Trypanosoma cruzi, enhance cellular invasion in vitro via activated TGF-β1. J Extracell Vesicles. 2024 Nov;13(11):e70014. doi: 10.1002/jev2.70014.

[12] Mannaperuma D, Stratton D, Lange S, Inal JM. Extracellular Vesicles from the Myocyte Secretome Contribute In Vitro to Creating an Unfavourable Environment for Migrating Lung Carcinoma Cells. Biology (Basel). 2025 Nov 11;14(11):1578. doi: 10.3390/biology14111578.

[13] DiNicolantonio JJ, O'Keefe JH, McCarty MF. Supplemental N-acetylcysteine and other measures that boost intracellular glutathione can downregulate interleukin-1β signalling: a potential strategy

for preventing cardiovascular events? Open Heart. 2017 Jul 28;4(2):e000599. doi: 10.1136/openhrt-2017-000599.

[14] Choezom D, Gross JC. Neutral sphingomyelinase 2 controls exosome secretion by counteracting V-ATPase-mediated endosome acidification. J Cell Sci. 2022 Mar 1;135(5):jcs259324. doi: 10.1242/jcs.259324.

[15] Welsh JA, Goberdhan DCI, O'Driscoll L, Buzas EI, Blenkiron C, Bussolati B, Cai H, Di Vizio D, Driedonks TAP, MISEV Consortium *et al.* Minimal information for studies of extracellular vesicles (MISEV2023): From basic to advanced approaches. J Extracell Vesicles. 2024 Feb;13(2):e12404. doi: 10.1002/jev2.12404.

[16] Trajkovic K, Hsu C, Chiantia S, Rajendran L, Wenzel D, Wieland F, Schwille P, Brügger B, Simons M. Ceramide triggers budding of exosome vesicles into multivesicular endosomes. Science. 2008 Feb 29;319(5867):1244-7. doi: 10.1126/science.1153124.

[17] Rutkute K, Asmis RH, Nikolova-Karakashian MN. Regulation of neutral sphingomyelinase-2 by GSH: a new insight to the role of oxidative stress in aging-associated inflammation. J Lipid Res. 2007 Nov;48(11):2443-52. doi: 10.1194/jlr.M700227-JLR200.

[18] Holopainen JM, Angelova MI, Kinnunen PK. Vectorial budding of vesicles by asymmetrical enzymatic formation of ceramide in giant liposomes. Biophys J. 2000 Feb;78(2):830-8. doi: 10.1016/S0006-3495(00)76640-9.

[19] Liu B, Hannun YA. Inhibition of the neutral magnesium-dependent sphingomyelinase by glutathione. J Biol Chem. 1997 Jun 27;272(26):16281-7. doi: 10.1074/jbc.272.26.16281.

[20] Lombardi M, Gabrielli M, Adinolfi E, Verderio C. Role of ATP in Extracellular Vesicle Biogenesis and Dynamics. Front Pharmacol. 2021 Mar 15;12:654023. doi: 10.3389/fphar.2021.654023.

[21] Bagrij T, Klokouzas A, Hladky SB, Barrand MA. Influences of glutathione on anionic substrate efflux in tumour cells expressing the multidrug resistance-associated protein, MRP1. Biochem Pharmacol. 2001 Jul 15;62(2):199-206. doi: 10.1016/s0006-2952(01)00660-8.

[22] Lombardi M, Gabrielli M, Adinolfi E, Verderio C. Role of ATP in Extracellular Vesicle Biogenesis and Dynamics. Front Pharmacol. 2021 Mar 15;12:654023. doi: 10.3389/fphar.2021.654023.

[23] Fraternale A, Zara C, De Angelis M, Nencioni L, Palamara AT, Retini M, Di Mambro T, Magnani M, Crinelli R. Intracellular Redox-Modulated Pathways as Targets for Effective Approaches in the Treatment of Viral Infection. Int J Mol Sci. 2021 Mar 30;22(7):3603. doi: 10.3390/ijms22073603.
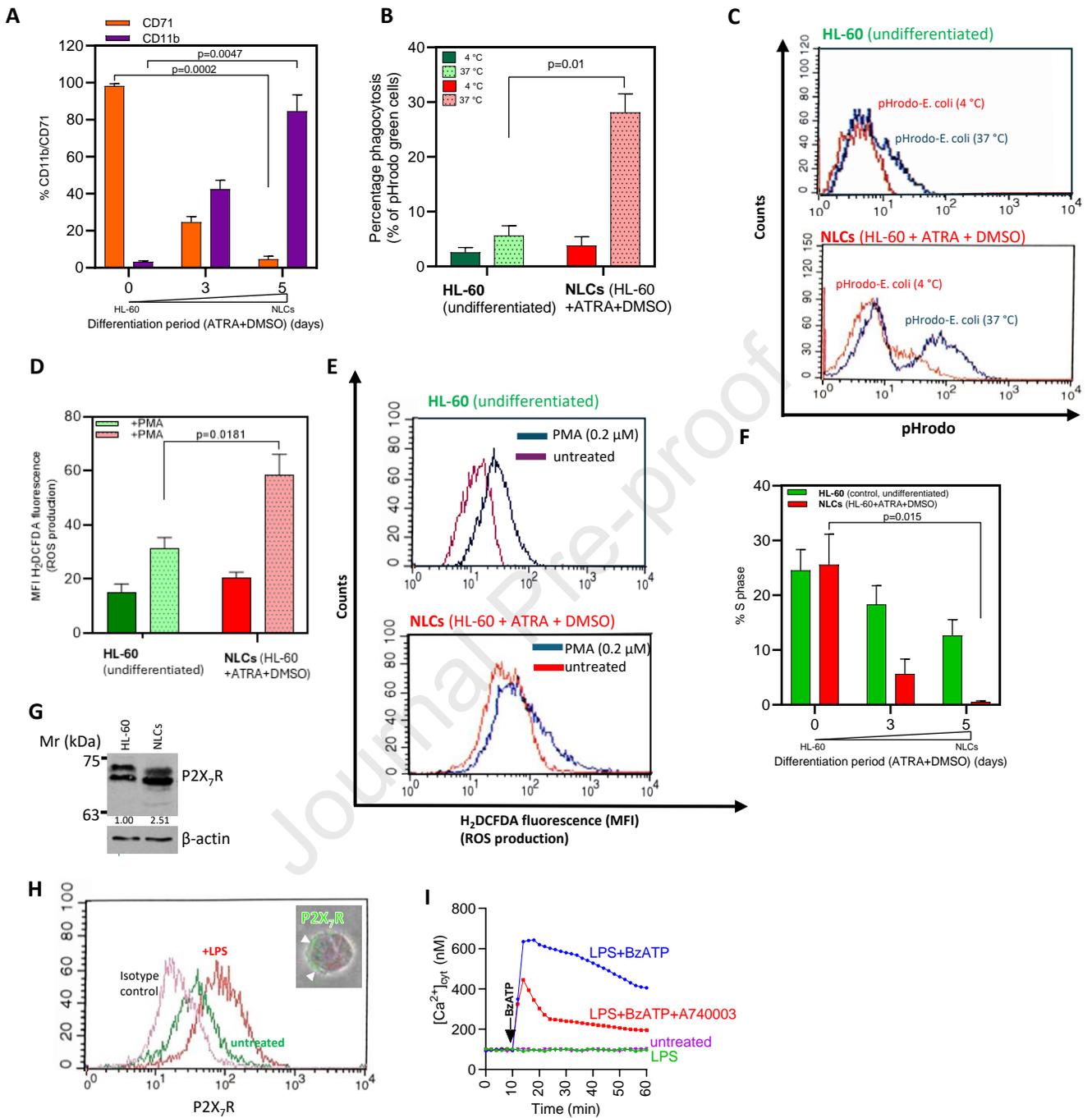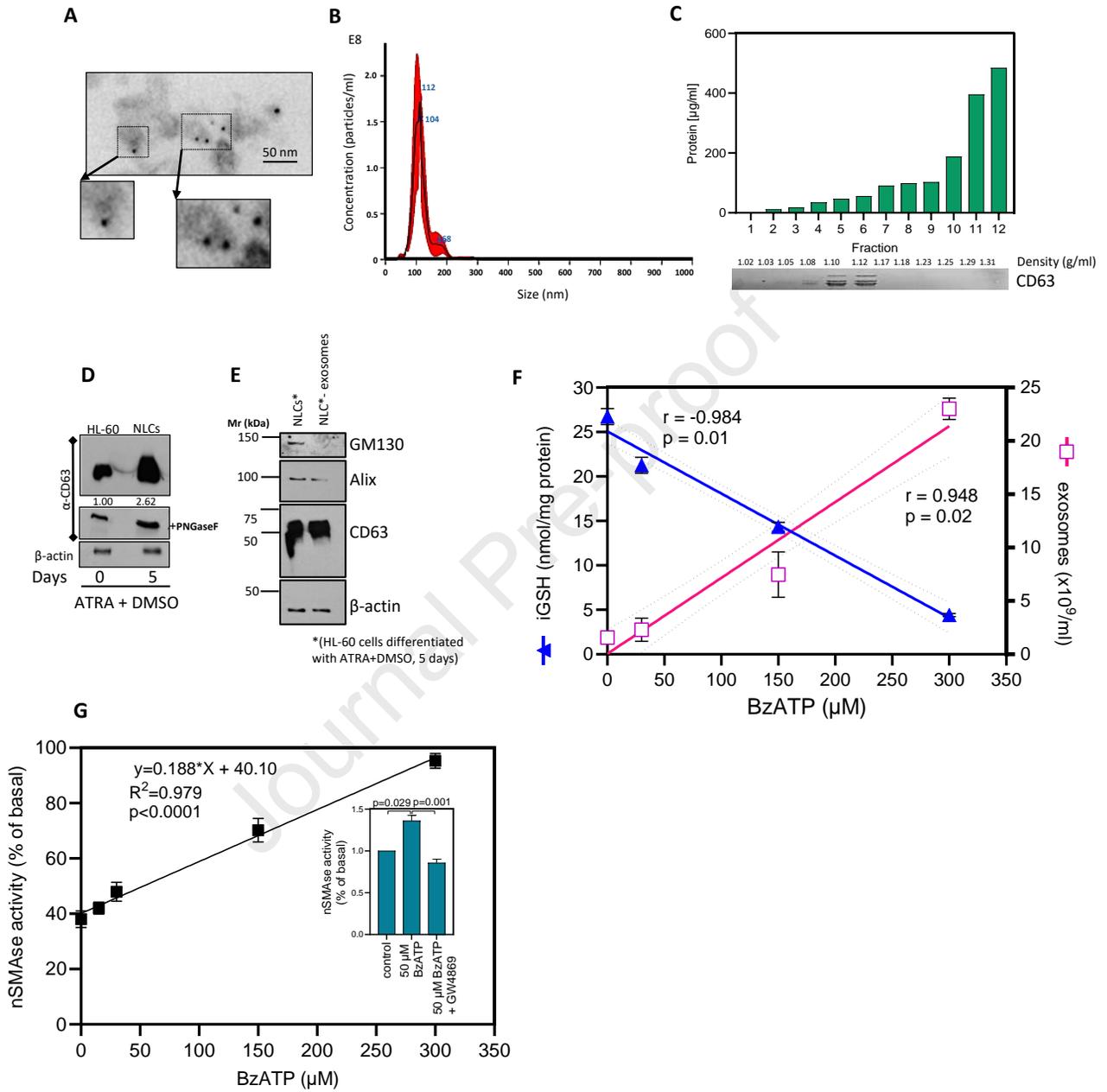
Fig. 1

Fig. 2

A

50 nm

B

E8

Concentration (particles/ml)

112
104
68

Size (nm)

C

Protein [µg/ml]

Fraction

Density (g/ml)
1.02 1.03 1.05 1.08 1.10 1.12 1.17 1.18 1.23 1.25 1.29 1.31

CD63

D

HL-60 NLCs

α-CD63

1.00 2.62

+PNGaseF

β-actin

Days 0 5

ATRA + DMSO

E

Mr (kDa)

NLCs*
NLC*- exosomes

150   GM130

100   Alix

75
       CD63
50

50   β-actin

*(HL-60 cells differentiated
with ATRA+DMSO, 5 days)

F

iGSH (nmol/mg protein)

exosomes (x10^9/ml)

r = -0.984
p = 0.01

r = 0.948
p = 0.02

BzATP (µM)

G

nSMAse activity (% of basal)

y=0.188*X + 40.10
R^2=0.979
p<0.0001

BzATP (µM)

nSMAse activity
(% of basal)

p=0.029 p=0.001

control
50 µM BzATP
50 µM BzATP + GW4869

Fig. 3

A

IC$_{50}$ = 10.34 μM [95% CI, 5.64-16.90]

p<0.0001

B

p=0.0116 p=0.0174

untreated control

MK-571

150 μM BzATP

C

p=0.042

p=0.049

- MK-571 - MK-2206

D

**** **** **** ****

* * **** **** ****

BzATP (μM)

■ BzATP
■ BzATP+ MK-571

E

ns ns **** ****

ns ns ns ** ****
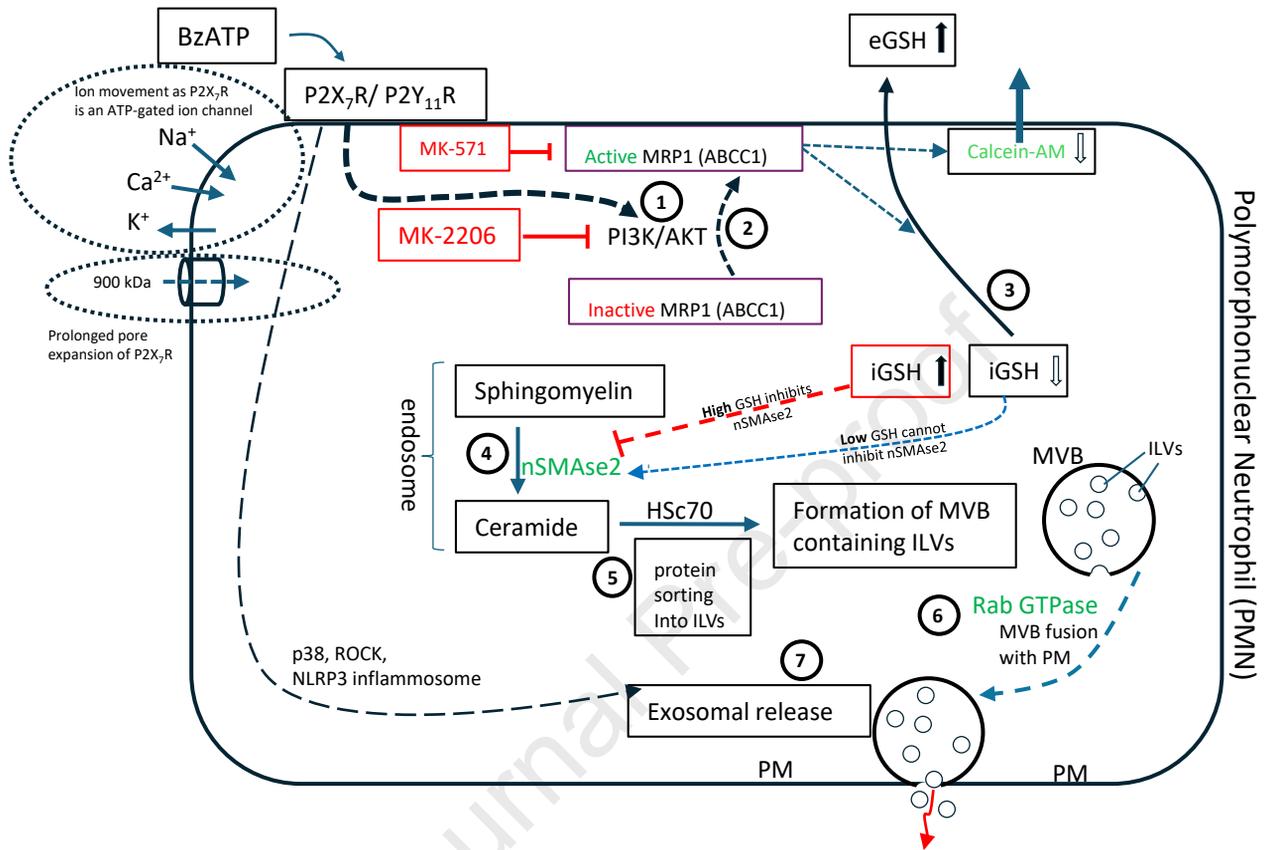
BzATP (μM)

■ BzATP
■ BzATP+ MK-571

Fig. 4

Highlights

- ATP triggers PI3K/AKT-MRP1-nSMase signaling in NLCs, causing rapid exosome release

- BzATP-induced, ceramide-dependent exosome release occurs via PI3K/AKT-MRP1/GSH axis

- Modulating neutrophil vesicles in inflammation using pathway and lipid targeting

Declaration of interests

The authors declare no known competing financial interests or personal relationships that could have appeared to influence the work reported in this paper.